Reaction mechanisms in the ^{6}Li+^{59}Co system

F.A. Souza, N. Carlin, R. Liguori Neto, M. M. de Moura, M. G. Munhoz, M. G. del Santo, A. A. P. Suaide, E. M. Szanto, A. Szanto de Toledo, C. Beck, et al.

Reaction mechanisms in the ^{6}Li+^{59}Co system

F. A . Souza [a,*,1], N. Carlin [a], R. Liguori Neto [a],

M. M. de Moura [a], M. G. Munhoz [a], M. G. Del Santo [a],

A. A. P. Suaide [a], E. M. Szanto [a], A. Szanto de Toledo [a],

C. Beck [b], N. Keeley [c,2]

[a] *Instituto de Física - Universidade de São Paulo, Departamento de Física Nuclear, C.P. 66318, 05315-970, São Paulo - SP, Brazil*

[b] *Institut Pluridisciplinaire Hubert Curien, UMR 7178, CNRS-IN2P3 et Université Louis Pasteur, Boîte Postale 28, F-67037 Strasbourg, Cedex 2, France*

[c] *CEA-Saclay DSM/IRFU/SPhN, F-91191 Gif sur Yvette Cedex, France*

Abstract

The reactions induced by the weakly bound ^{6}Li projectile interacting with the intermediate mass target ^{59}Co were investigated. Proton, deuteron and α-particle singles measurements were performed at the near barrier energies E_{lab} = 17.4, 21.5, 25.5 and 29.6 MeV. The main contributions of the different competing mechanisms are discussed. A statistical model analysis, Continuum-Discretized Coupled-Channels calculations and two-body kinematics were used as tools to provide information to disentangle the main components of these mechanisms.

PACS: 25.70.Jj; 25.70.Mn; 25.70.Gh; 24.10.Eq

Keywords: Complete fusion; Incomplete fusion; Breakup; Transfer; Two-body kine-

1 Introduction

Experiments with heavy ions performed during the last decade have shown that the internal degrees of freedom of the interacting nuclei play an important role in determining the reaction flux diverted toward the fusion reaction [1–6]. Barrier distribution measurements [3] have shown that the coupling of collective degrees of freedom to the fusion channel may enhance the sub-barrier total fusion cross section. Interest in fusion studies at near- and sub-barrier energies with exotic nuclei as projectiles [5–13] has been renewed with the recent increased availability of Radioactive Ion Beams (RIB). The investigation of such reactions involving unstable nuclei, far from the valley of stability, should have a great impact on the study of astrophysical processes at very low bombarding energies near the Gamow peak [13,14]. Light unstable nuclei display low nucleon (cluster) separation energies, and are therefore candidates for important breakup (BU) cross sections. This possibility affects the dynamics of fusion reactions [15–22] due to the fact that part of the incoming flux may be lost from the entrance channel before overcoming the fusion barrier and, moreover, one of the fragments removed from the projectile (or target) may fuse leading to an important incomplete fusion (ICF) or transfer (TR) contribution. The contributions of these reaction mechanisms have not so far

* Corresponding author.
Email address: fsouza@dfn.if.usp.br (F. A . Souza).
[1] phone: 55-11-3091-6939 fax: 55-11-3031-2742
[2] Permanent address: Department of Nuclear Reactions, The Andrzej Sołtan Institute for Nuclear Studies, ul. Hoża 69, PL-00681 Warsaw, Poland

been identified in barrier distribution measurements or clearly disentangled in "singles" evaporated particle measurements. Angular correlation measurements are required to guarantee the occurrence of BU processes in order to shed some light on the understanding of this problem which remains controversial as conflicting theoretical expectations have been reported in the recent past [23–31].

We have already performed measurements for ^{6,7}Li beams incident on the intermediate-mass target ^{59}Co at near barrier energies and studied the total fusion [32], elastic scattering [33] and BU cross sections [34]. In this work we present a study of the inclusive light charged particle spectra for the ^{6}Li + ^{59}Co system and the respective contributions of the different mechanisms are discussed. Measurements were performed at four bombarding energies above the Coulomb barrier ($V_B = 12.0$ MeV). Experimental details are given in Sec. 2. A statistical-model analysis and two-body kinematics, presented in Sec. 3, were used as tools to distinguish the CF, ICF, TR and BU components and to provide information on their respective properties. Sec. 3 proposes a discussion of the cross section balance assuming that the BU yield can be estimated within the Continuum-Discretized Coupled-Channels (CDCC) approach [28–31].

2 Experimental details

The experiments were performed at the University of São Paulo Physics Institute. The ^{6}Li beam was delivered by the 8UD Pelletron accelerator with energies $E_{lab} = 18,\ 22,\ 26$ and 30 MeV, and bombarded a 2.2 mg/cm^2 thick ^{59}Co target. Due to the target thickness the bombarding energies were cor-

rected for the energy loss at the center of the target. The corrected energies are $E_{lab} = 17.4,\ 21.5,\ 25.5$ and 29.6 MeV, respectively.

Light charged particles (LCP) emitted during the ^{6}Li + ^{59}Co reaction were detected by means of 11 triple telescopes [35] separated by $\Delta\theta = 10^{\circ}$ and installed in the reaction plane. The triple telescopes were composed of an ionization chamber (ΔE_1) followed by a 150 μm Si(SB) detector (ΔE_2) and a 40 mm CsI crystal (E) with photodiode readout to measure the LCP residual energy. The entrance window of the ionization chamber ΔE_1 was a 150 μg/cm^2 aluminized polypropylene film. The use of 20 torr isobutane in the ionization chambers allowed an energy resolution of 7.6% in the ΔE_1 signal to be achieved.

Particle identification of the LCPs emitted during the reaction was achieved by means of two-dimensional spectra of the ΔE_1, ΔE_2 and E signals processed by means of standard NIM and CAMAC electronics. The energy loss in each detector was calculated using a universal analytic equation [36]. The ΔE_{gas} and E_{heavy} signals were calibrated using the ^{6}Li elastic scattering peaks. The curves of the residual energy deposited in the CsI crystal as a function of energy loss in the Si detector for each Z and the linear relation between the E_{heavy} and ΔE_{light} gains were used to calibrate the energy spectra of the LCPs. The telescopes covered the angular range from $\theta = -45^{\circ}$ to $\theta = -15^{\circ}$ and from $\theta = 15^{\circ}$ to $\theta = 75^{\circ}$, both in $\Delta\theta = 10^{\circ}$ steps. The solid angles of the telescopes varied from $\Delta\Omega = 0.14$ to $\Delta\Omega = 1.96$ msr. Absolute cross-sections were determined from our earlier elastic scattering measurements [33].

3 Results and discussion

For reactions induced by the weakly bound projectile ^{6}Li ($Q = -1.47$ MeV for the $\alpha + d$ breakup) it is natural to assume that the main contributor to the α and d yields is the $\alpha + d$ breakup, but other processes are also likely to occur with significant significant cross sections [22]. The processes we take into account are the following:

a) $^6\mathrm{Li} + {}^{59}\mathrm{Co} \rightarrow {}^6\mathrm{Li}^* + {}^{59}\mathrm{Co} \rightarrow \alpha + d + {}^{59}\mathrm{Co}$

b) $^6\mathrm{Li} + {}^{59}\mathrm{Co} \rightarrow \alpha + {}^{61}\mathrm{Ni}^* \rightarrow$ subsequent decay

c) $^6\mathrm{Li} + {}^{59}\mathrm{Co} \rightarrow d + {}^{63}\mathrm{Cu}^* \rightarrow$ subsequent decay

d) $^6\mathrm{Li} + {}^{59}\mathrm{Co} \rightarrow {}^5\mathrm{Li} + {}^{60}\mathrm{Co}^* \rightarrow$ subsequent decay

e) $^6\mathrm{Li} + {}^{59}\mathrm{Co} \rightarrow {}^5\mathrm{He} + {}^{60}\mathrm{Ni}^* \rightarrow$ subsequent decay

f) $^6\mathrm{Li} + {}^{59}\mathrm{Co} \rightarrow {}^{65}\mathrm{Zn}^* \rightarrow$ subsequent decay

Process a) is identified as the breakup of ^{6}Li, which could be either direct or resonant (sequential). In this case there is no further capture of the BU products by the target; we will call it non-capture breakup (NCBU). Process b) is identified as either ICF of d+^{59}Co (d-ICF) after BU or a direct one-step d transfer (d-TR), both with subsequent decay of the excited ^{61}Ni*. Here, the α particle is left as a "spectator". In the same way, process c) can be identified as either ICF of α+^{59}Co (α-ICF) after BU or a direct one-step α transfer (α-TR), both with subsequent decay of the excited ^{63}Cu*. In this case the d is left as

a "spectator". Processes d) and e) represent single neutron and single proton stripping from the ^{6}Li projectile, respectively with subsequent decay of the unstable ^{5}Li and ^{5}He leaving an α particle plus a neutron or proton. Process f) is simply identified as complete fusion (CF). In all processes involving deuteron emission in the exit channel subsequent breakup of the deuteron was not taken into account, in accordance with Refs. [37,38].

Our experimental setup allowed us to obtain LCP singles and coincidence data. For instance, the $\alpha - d$ coincidence data could have a contribution from NCBU as well as coincidences between a light quasi-projectile fragment and a LCP from an ICF/TR decay process. A contribution from CF decay is also possible. However, in this work we will concentrate on the results obtained from the analysis of the LCP singles data.

In figures 1a and 1b we show sample singles p and α production spectra (chosen among the spectra for the various energies and angles) together with statistical-model predictions for CF decay using the Hauser-Feshbach evaporation code CACARIZO [39,40] (the Monte Carlo version of CASCADE [40]). In the calculations the transmission coefficients were evaluated using optical model (OM) parameters for spherical nuclei. The compound nucleus (CN) angular momentum distributions were specified using the diffuseness parameter $\Delta L = 1$ and the critical angular momentum L_{crit} calculated internally by the code for each bombarding energy. The OM potentials for n, p, and α were taken from Rapaport *et al.* [41], Perey [42], and Huizenga and Igo [43], respectively. One of the most important parameters in the calculations is the level density parameter a. In our case it was defined as $a_{LDM} = A/10$ [44] rather than the A/8 value adopted for other systematic studies [40]. This value of a, needed to reproduce the Giant Dipole Resonance (GDR) enhancement in the

^{6}Li + ^{57}Fe γ-ray spectra [44], provided good results for the LCP energy spectra without any extra normalization on the CF cross-sections. In particular, the proton energy spectra for which we expect essentially CN decay (except in the low-energy region where p decay from ICF and TR intermediate nuclei might be apparent; protons from d breakup were not considered, as already argued) were very well reproduced for all detection angles (as shown in figure 1a). We performed additional CACARIZO calculations for d- and α-ICF assuming bombarding energies corresponding to the ^{6}Li projectile velocity. The location of the p decay energies supports well this rather crude hypothesis.

In figure 1b we note that there is clearly a contribution from other mechanisms in the α-production spectra. In this case, after subtraction of the contribution from the CF α particles as calculated by CACARIZO, two "bumps" remain, as can be seen in figure 2a. This figure displays energy spectra at $\theta = 45^{\circ}$ for $E_{lab} = 21.5$ MeV. Very similar spectra (not shown) were recorded at the three other bombarding energies. In figure 2a the small low-energy bump is attributed to decay of ICF and TR intermediate nuclei. This attribution is supported by the results of the CACARIZO calculations for d and α-ICF. The high-energy bump is the subject of the analysis that follows.

For the high-energy α-bump, according to the description above, we are then dealing with the experimental quantity $\sigma_{\alpha-bump}$ defined as:

$$\sigma_{\alpha-bump} = \sigma_{d-ICF} + \sigma_{d-TR} + \sigma_{NCBU} + \sigma_{n-TR} + \sigma_{p-TR} \quad (1)$$

Analogously for the d singles energy spectra, shown in figure 2b, we may define the quantity σ_{d-bump} as:

$$\sigma_{d-bump} = \sigma_{\alpha-ICF} + \sigma_{\alpha-TR} + \sigma_{NCBU} \quad (2)$$

The quantities $\sigma_{\alpha-bump}$ and σ_{d-bump} were obtained through the integration of the angular distributions (dashed lines) shown in figures 2c and 2d, respectively. In the same figures we present experimental α and d angular distributions for $E_{lab} = 21.5$ MeV. As we only have data points up to $\theta = 75^{\circ}$ we have assumed that the total α and d production at backward angles is essentially due to CF and ICF/TR decays. In order to estimate the shape of the angular distribution for the backward angles we used CACARIZO predictions for the CF decay. The adopted shapes are consistent with published data for ^{6}Li + ^{58}Ni at similar bombarding energies [45].

In figure 3 we present an excitation function, adopted from [45,46], of total α production cross section as a function of reduced energy for ^{6}Li on various targets at near and above barrier energies [22,45,46]. As noted in [46], a simple systematic behavior for total α production is observed with no significant target dependence. We also include the present results for ^{6}Li + ^{59}Co, obtained from the integration of the angular distributions (i.e. the solid curve in figure 2c and its counterparts at the other incident energies). The Coulomb barrier ($V_B = 12.0$ MeV) was extracted from Ref. [32]. We note that the ^{6}Li + ^{59}Co data also obey the systematic trend giving further support to the present analysis. It is worth noting that a similar trend has been obtained for ^{7}Li projectiles [47]. The dashed line plotted in the figure displays the excitation function of α particles calculated by CACARIZO for ^{6}Li + ^{59}Co, i.e. those α particles that are emitted through a fusion-evaporation process. As the experimental data (stars) lie well above the fusion predictions we may conclude that the ICF and TR components both play a significant role in the total α production. This behavior is even stronger for ^{6}He induced reactions [7,9,10,48] for which the measured total α cross sections are much larger than for ^{6}Li due

to the strong competition of the 1n- and 2n-transfer reactions as convincingly demonstrated in the ^{6}He + ^{209}Bi system [49,50], for instance.

A clear separation of mechanisms involves a knowledge of the σ_{NCBU} cross-section. In this work we adopted the approach of performing CDCC [28–31] calculations to evaluate σ_{NCBU}. The exclusive BU cross-sections for the resonant states in ^{6}Li plus the non-resonant α+d continuum were calculated using a cluster-folding model with potentials that describe well the measured elastic scattering angular distributions [29–31]. The CDCC calculations for ^{6}Li were performed with the code FRESCO assuming an $\alpha + d$ cluster structure, similar to that described in [28,29]. The $\alpha + d$ binding potentials were taken from [51] and couplings to the 3^+ ($E^* = 2.18$ MeV), 2^+ ($E^* = 4.31$ MeV) and 1^+ ($E^* = 5.65$ MeV) resonant states were included as well as couplings to the non-resonant $\alpha + d$ continuum. The continuum was discretized into a series of momentum bins of width $\delta k = 0.2$ fm^{-1} with maximum $k = 1$ fm^{-1}, where $\hbar k$ denotes the momentum of the $\alpha + d$ relative motion. In order to avoid double counting the width δk was suitably modified in the presence of resonances. In the calculations each momentum bin was treated as an excited state of ^{6}Li, at an excitation energy equal to the mean energy of the bin and having spin $\vec{I}$ and parity $(-1)^L$. The angular momenta are related by $\vec{I} = \vec{L} + \vec{s}$, where $\vec{s}$ is the spin of the d and $\vec{L}$ is the relative angular momentum of $\alpha + d$ cluster system. Following Hirabayashi [52] couplings to states with $L \geq 3$ are expected to be small. Thus, L was limited to 0, 1, 2, 3. All couplings, including continuum-continuum couplings, up to multipolarity $\lambda = 3$ were included. Details of the CDCC method may be found in Refs. [28–31,53].

In Table 1 we present a summary of our results obtained from the experimental LCP singles spectra and the evaluation of non-capture BU (NCBU)

cross sections with CDCC [29]. The CACARIZO predictions for the CF α evaporation channel ($\sigma_{\alpha}^{total} - \sigma_{\alpha-bump}$, excluding NCBU) may be compared with the results obtained in our work reporting total fusion measurements for ^{6}Li+^{59}Co [32]. Although in that work [32] we had in some cases a mixture of channels (CF and ICF for instance) due to the limitations of the gamma-ray spectroscopy method, the values are in relatively good agreement, to within 30%. The total reaction cross sections were extracted from our elastic scattering analysis [33] using the São Paulo Potential [54] and from the CDCC calculations [29]. The OM fits and the CDCC calculations yield similar cross sections which are much larger than the total fusion cross sections [32] measured at $E_{lab} = 17.4$ MeV and $E_{lab} = 25.5$ MeV using the gamma-ray method [32]. Let us recall that the measured total fusion cross sections were also found to be quite well reproduced by the CDCC method [28].

When comparing the values of $\sigma_{\alpha-bump}$ and σ_{d-bump} in Table 1 we note that there is an excess of α particles over d (approximately a factor of 3). This behavior for a ^{59}Co target confirms that found previously for ^{58}Ni and ^{118,120}Sn targets [45] at similar bombarding energies. Since the Coulomb barrier for d-ICF/TR is lower than that for α-ICF/TR, we would expect a larger α yield than d yield. Single nucleon transfer reactions will also produce α particles but not deuterons, and thus could also contribute to the excess of α particles over deuterons. Although a full calculation of these processes is not possible for a ^{59}Co target due to the high density of states in the residual target-like nuclei, DWBA estimates suggest that the single nucleon transfer cross sections are at least as large as those for NCBU [29]. A similar excess of α particles over d has also been reported previously in the literature for other systems, not only for energies similar to ours [45] but also at higher energies [37,55].

The results presented in Table 1 (note that the CDCC cross sections reported in Table I were obtained by interpolation of the values calculated at 18, 26, and 30 MeV in Ref. [29]) show that the NCBU cross section is significantly lower than the $\sigma_{\alpha-bump}$ and σ_{d-bump} cross sections. This is also observed in other recent work [29]. In this case we could argue that the main contributions to $\sigma_{\alpha-bump}$ and σ_{d-bump} are most probably due to both the ICF and TR mechanisms.

In order to confirm whether our assumption is reasonable we performed a two-body kinematics analysis related to the centroids of the high-energy α-bump and d-bump as a function of the detection angle. For the sake of simplicity we have not considered three-body kinematics calculations which would have to be performed for the TR processes labeled d) and e). If the ICF and TR mechanisms are dominant the energy corresponding to the centroids should reflect the excitation energy of the ^{61}Ni* and ^{63}Cu* nuclei formed in the intermediate stage of processes b) and c) described above, as they are two-body processes. In figure 4 we show the behavior of the energy associated with the centroids of the high-energy α-bump and the d-bump for all bombarding energies. We also present two-body kinematics calculations for the α and d energies as a function of the detection angle for fixed excitation energies of the intermediate nuclei ^{61}Ni* and ^{63}Cu*. The uncertainty in the particle energy corresponds to the uncertainty in the determination of the total energy ($\sim$ 0.5 MeV). The different curves in figure 4 represent the behavior for the excitation energies of the intermediate nuclei that provided the best fits to the experimental results. The uncertainty associated with the fits is approximately 0.5 MeV. The good agreement with the experimental results suggests that our assumption about the mechanisms is reasonable.

Considering the experimental uncertainties the excitation energies obtained are consistent with an ICF process for which the α and d have approximately the projectile velocity. The calculated values are shown between parentheses in figure 4. On the other hand, if we consider the TR process the agreement between the best experimental excitation energies and the ones obtained from optimum Q-value calculations [56] (shown between brackets in figure 4) is not as good as for the ICF case. However, due to the existence of different relations for calculating optimum Q-values we cannot a priori rule out the contribution of the TR processes labelled d) and e). The neutron TR contribution, for instance, has been found to be a rather competitive reaction channel in the ^{6}Li + ^{118}Sn and ^{6}Li + ^{208}Pb reactions [57] as well as in the ^{6}Li + ^{28}Si reaction [38]. It is worth noting that following Ref. [37,38] we did not consider the secondary disintegration of the deuterons, the contribution of which is expected to be much smaller [37].

From this analysis we conclude that the main contributions to the α-bump and d-bump are due to both ICF and TR. However, it was not possible to disentangle their individual contributions from the present inclusive data. This is one of the present challenges for investigations involving systems with weakly bound nuclei and exclusive measurements would help in this respect.

4 Conclusions

In this work we presented results for the intermediate mass target ^{6}Li + ^{59}Co reaction involving the weakly bound ^{6}Li. Proton, deuteron and α particle inclusive measurements were performed at the near barrier energies E_{lab} = 17.4, 21.5, 25.5 and 29.6 MeV. The contributions of different LCP production

mechanisms were discussed. A statistical-model analysis, CDCC calculations and two-body kinematics were used as tools to provide information on the competing processes.

The analysis of the high-energy α-bump and d-bump, obtained after the subtraction of the CF decay contribution, suggests that the main contribution to the high-energy α-bump and d-bump cross sections is a combination of the ICF and TR mechanisms, as the non-capture BU cross section is estimated to be relatively small according to CDCC calculations. This assumption is confirmed firstly by the total α production, which is much more intense than predictions using the statistical model, and secondly by a two-body kinematics analysis. In this work it was not possible to fully disentangle the individual ICF and TR contributions. A clear separation of the different reaction mechanisms remains one of the main challenges in the study of fusion reactions induced by weakly bound nuclei. To achieve this goal and to better constrain the different theoretical approaches (such as CDCC) more complete and exclusive measurements will be needed in the near future.

Acknowledgements

The authors thank FAPESP and CNPq for financial support. N.K. gratefully acknowledges the receipt of a Marie Curie Intra-European Fellowship from the European Commission, contract No. MEIF-CT-2005-010158. We would also like to thank A. Pakou, A. M. Moro and C. Signorini for their careful reading of the manuscript.

References

[1] A. B. Balantekin and N. Takigawa, Rev. Mod. Phys. 70 (1998) 77.

[2] J. Al-Khalili and F. Nunes, J. Phys. (London) G 29 (2003) R89.

[3] M. Dasgupta, D. J. Hinde, N. Rowley, and A. M. Stefanini, Annu. Rev. Nucl. Part. Sci. 48 (1998) 401.

[4] L. F. Canto, P. R. S. Gomes, R. Donangelo and M. S. Hussein, Phys. Rep. 424 (2006) 1.

[5] N. Keeley, R. Raabe, N. Alamanos, and J.L. Sida, Prog. Part. Nucl. Phys. 59 (2007) 579.

[6] J. F. Liang and C. Signorini, Int. Jour. of Modern Physics E 14 (2006) 1121.

[7] J. J. Kolata, et al., Phys. Rev. Lett. 81 (1998) 4580.

[8] E. F. Aguilera, et al., Phys. Rev. Lett. 84 (2000) 5058.

[9] R. Raabe, et al., Nature 431 (2004) 823.

[10] A. Di Pietro, et al., Phys. Rev. C 69 (2004) 044613.

[11] A. Navin, et al., Phys. Rev. C 70 (2004) 044601.

[12] Yu. E. Penionzhkevich, et al., Eur. Phys. Jour. A 31 (2007) 185.

[13] K. E. Rehm, et al., Phys. Rev. Lett. 81 (1998) 3341.

[14] M. S. Smith and K. E. Rehm, Annu. Rev. Nucl. Part. Sci. 51 (2001) 91.

[15] M. Dasgupta, et al., Phys. Rev. Lett. 82 (1999) 1395.

[16] V. Tripathi, et al., Phys. Rev. Lett. 88 (2002) 172701.

[17] G. V. Marti, et al., Phys. Rev. C 71 (2005) 027602.

[18] P. R. S. Gomes, et al., Phys. Rev. C 71 (2005) 017601.

[19] A. Shrivastava, et al., Phys Lett. B 633 (2006) 463.

[20] A. Pakou, et al., Phys. Lett. B 633 (2006) 691.

[21] P. R. S. Gomes, et al., Phys. Lett. B 634 (2006) 356.

[22] C. Signorini, et al., Phys. Rev. C 67 (2003) 044607.

[23] N. Takigawa and H. Sagawa, Phys. Lett. B 265 (1991) 23.

[24] M. S. Hussein, M. P. Pato, L. F. Canto, and R. Donangelo, Phys. Rev. C 46 (1992) 377.

[25] C. H. Dasso and A. Vitturi, Phys. Rev. C 50 (1994) R12.

[26] K. Hagino, A. Vitturi, C.H. Dasso, and S. M. Lenzi, Phys. Rev. C 61 (2000) 037602.

[27] R. S. Mackintosh and N. Keeley, Phys. Rev. C 70 (2004) 024604.

[28] A. Diaz-Torres, I. J. Thompson, and C. Beck, Phys. Rev. C 68 (2003) 044607.

[29] C. Beck, N. Keeley and A. Diaz-Torres, Phys. Rev. C 75 (2007) 054605.

[30] C. Beck, Nucl. Phys. A 787 (2007) 251.

[31] C. Beck, A. Sànchez i Zafra, A. Diaz-Torres, I. J. Thompson, N. Keeley, and F. A. Souza, AIP Conferences Proceedings 853 (2006) 384; Fusion06 Conference, San Servolo, Venezia, Italy, 19-23 March 2006; arXiv:nucl-th/0605029v2.

[32] C. Beck, et al., Phys. Rev. C 67 (2003) 054602.

[33] F. A. Souza, et al., Phys. Rev. C 75 (2007) 044601.

[34] F. A. Souza, et al., Progr. Theor. Phys. Suppl. 154 (2004) 101.

[35] M. M. de Moura, et al., Nucl. Instr. Meth. A 471 (2001) 368.

[36] E. C. Montenegro, S. A. Cruz and C. Vargas-Aburto, Phys. Lett. A 92 (1982) 195.

[37] R. Ost, et al., Phys. Rev. C 5 (1972) 1835.

[38] A. Pakou, et al. Phys. Rev. C 76 (2007) 054601.

[39] G. Viesti, et al., Phys. Rev. C 38 (1988) 2640.

[40] D. Mahboub, et al., Phys. Rev. C 69 (2004) 034616.

[41] J. Rapaport, et al., Nucl Phys. A 330 (1979) 15.

[42] F. G. Perey, Phys. Rev. 131 (1963) 745.

[43] J. R. Huizenga and G. Igo, Nucl. Phys. 29 (1961) 462.

[44] M. Kicinska-Habior, et al., Phys. Rev. C 36 (1987) 612.

[45] K. O. Pfeiffer, E. Speth and K. Bethge, Nucl. Phys. A 206 (1973) 545.

[46] A. Pakou, et al., Phys. Rev. Lett. 90 (2003) 202701.

[47] A. Pakou, et al., Phys. Rev. C 71 (2005) 064602.

[48] D. Escrig, et al., Nucl. Phys. A 792 (2007) 2.

[49] J.P. Bychowski, et al., Phys. Lett. B 596 (2004) 62.

[50] P. A. de Young, et al., Phys. Rev. C 71 (2005) 051601R.

[51] K. I. Kubo and M. Hirata, Nucl. Phys. A187 (1972) 186.

[52] Y. Hirabayashi, Phys. Rev. C 44 (1991) 1581.

[53] C. Beck, et al., arXiv:0709.0439.

[54] M. A. G. Alvarez, L. C. Chamon, M. S. Hussein, D. Pereira, L. R. Gasques, E. S. Rossi, Jr.m and C. P. Silva., Nucl. Phys. A 723 (2003) 93.

[55] C. M. Castaneda, et al., Phys. Rev. C 21 (1980) 179.

[56] P. J. Siemens, et al., Phys. Lett. B 36 (1971) 24.

[57] D. Scholz, H. Gemmeke, L. Lassen, R. Ost, and K. Bethge, Nucl. Phys. A 288 (1977) 351.

Fig. 1. Experimental p (a) and α (b) singles spectra at $\theta = 45^\circ$ for $E_{lab} = 21.5$ MeV and the respective CACARIZO predictions (histograms) for the CF decay. The error bars are of the same size or smaller than the symbols used to represent the experimental points.

Fig. 2. (a) Experimental α singles energy spectrum (open circles) and α-bump (full circles) at $\theta = 45^\circ$ for $E_{lab} = 21.5$ MeV, obtained after subtracting the contribution of CF decay (dotted line). (b) The same for d. (c) Angular distribution for the total α production (open circles) and high-energy α-bump (full triangles). (d) The same for d. The solid and dashed lines correspond to the shapes adopted for the integration of the angular distributions. The dotted line in (c) and (d) is the CACARIZO prediction for CF decay. In most cases the error bars are of the same size or smaller than the symbols used to represent the experimental points.

Fig. 3. Total α production cross sections in reactions involving ^{6}Li on various targets as a function of the center of mass energy divided by the Coulomb barrier energy. We incorporate results extracted from [46] and [45]. We also include our results for ^{6}Li + ^{59}Co, which reproduce well the universal behavior of α production. The dashed line indicates the cross sections for α particles evaporated during the ^{6}Li + ^{59}Co CF process as simulated by the CACARIZO evaporation code.

Fig. 4. Energy of the centroids of the α-bump and d-bump as a function of the detection angle for all bombarding energies. The curves are two-body kinematics results and represent the behavior for the excitation energies of the intermediate nuclei that provided the best fits to the experimental results. The values between parentheses are the calculated excitation energies for the intermediate nuclei formed in an ICF process. The values between brackets are the calculated excitation energies for the intermediate nuclei formed in a TR process.

Table 1

Summary of the results obtained from our analysis, showing for all the bombarding energies the total α and d cross sections and the yields extracted from the α-*bump* and *d-bump*, respectively. Experimental total fusion cross sections [32], total reaction cross sections from OM fits [33] and CDCC calculations [29] as well as the non-capture BU cross sections evaluated with CDCC calculations [29] are also given.

E_{lab} (MeV)	σ_{α}^{total} (mb)	σ_{d}^{total} (mb)	$\sigma_{\alpha-bump}$ (mb)	σ_{d-bump} (mb)
17.4	404(22)	86(8)	243(36)	72(12)
21.5	560(14)	140(10)	319(38)	107(13)
25.5	715(29)	175(15)	332(33)	126(15)
29.6	843(35)	217(15)	322(23)	150(18)

E_{lab} (MeV)	$\sigma_{fus}^{\exp}$ (mb)	$\sigma_{Reac}^{\mathrm{OM}}$	$\sigma_{Reac}^{\mathrm{CDCC}}$ (mb)	$\sigma_{NCBU}^{\mathrm{CDCC}}$ (mb)
17.4	467(94)	780	943	33.6
21.5	-	1099	1243	44.9
25.5	988(199)	1368	1430	54.7
29.6	-	1540	1559	61.2

Figure 1

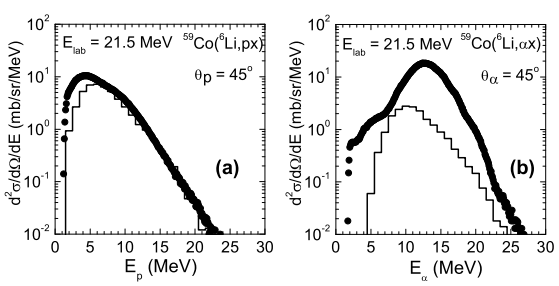
E_lab = 21.5 MeV
59Co(6Li,px)
θp = 45°
(a)
d²σ/dΩ/dE (mb/sr/MeV)
Ep (MeV)
E_lab = 21.5 MeV
59Co(6Li,αx)
θα = 45°
(b)
Eα (MeV)

Figure 2

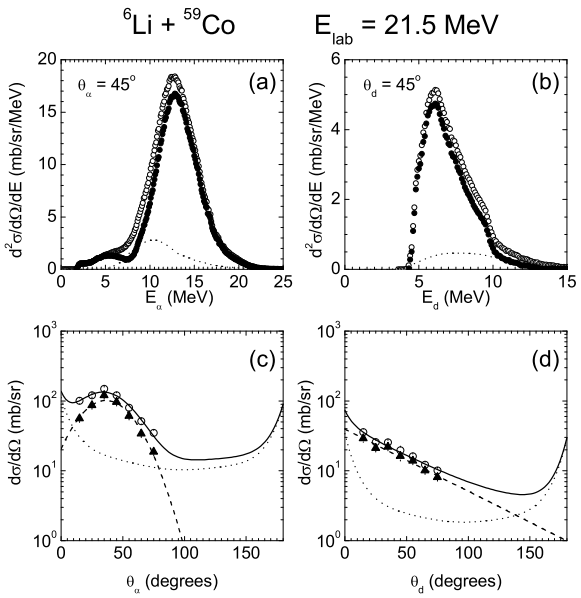
^{6}Li + ^{59}Co
E_{lab} = 21.5 MeV
θ_α = 45°
(a)
$d^2\sigma/d\Omega/dE$ (mb/sr/MeV)
E_α (MeV)
θ_d = 45°
(b)
$d^2\sigma/d\Omega/dE$ (mb/sr/MeV)
E_d (MeV)
(c)
$d\sigma/d\Omega$ (mb/sr)
θ_α (degrees)
(d)
$d\sigma/d\Omega$ (mb/sr)
θ_d (degrees)

Figure 3

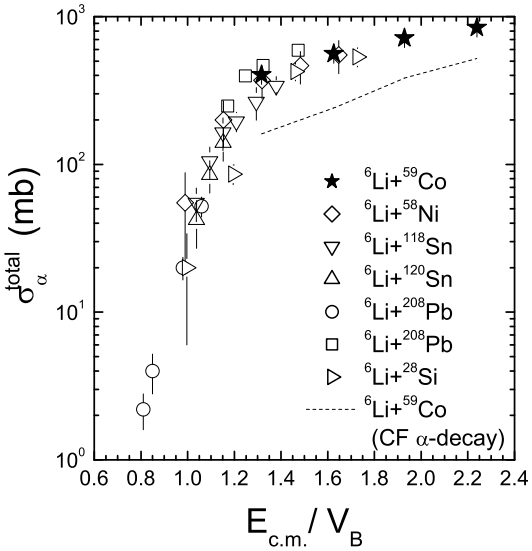
10^3
10^2
10^1
10^0
σ_α^{total} (mb)
0.6 0.8 1.0 1.2 1.4 1.6 1.8 2.0 2.2 2.4
$E_{c.m.} / V_B$
^{6}Li+^{59}Co
^{6}Li+^{58}Ni
^{6}Li+^{118}Sn
^{6}Li+^{120}Sn
^{6}Li+^{208}Pb
^{6}Li+^{208}Pb
^{6}Li+^{28}Si
^{6}Li+^{59}Co
(CF α-decay)

Figure 4

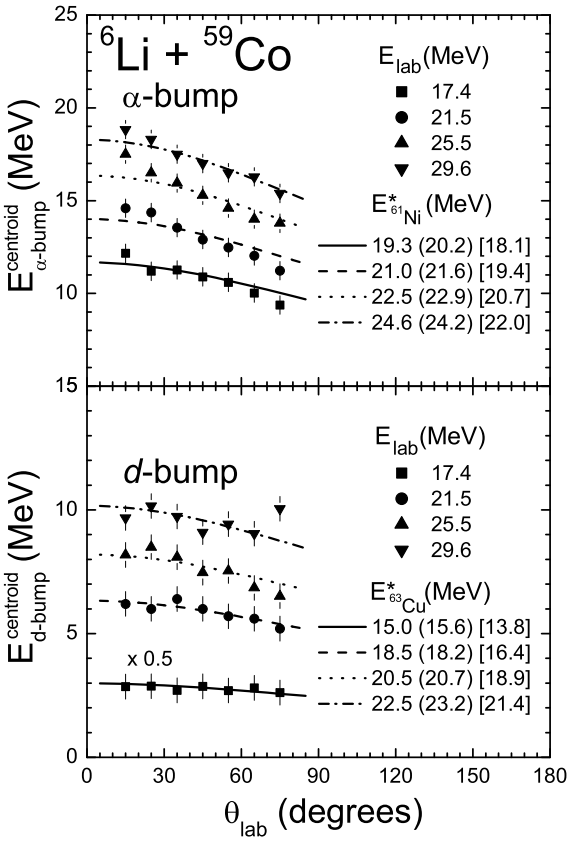
^{6}Li + ^{59}Co
α-bump
$E^{centroid}_{α-bump}$ (MeV)
E_{lab}(MeV)
17.4
21.5
25.5
29.6
$E^{*}_{^{61}Ni}$(MeV)
19.3 (20.2) [18.1]
21.0 (21.6) [19.4]
22.5 (22.9) [20.7]
24.6 (24.2) [22.0]
d-bump
$E^{centroid}_{d-bump}$ (MeV)
E_{lab}(MeV)
17.4
21.5
25.5
29.6
$E^{*}_{^{63}Cu}$(MeV)
15.0 (15.6) [13.8]
18.5 (18.2) [16.4]
20.5 (20.7) [18.9]
22.5 (23.2) [21.4]
x 0.5
$θ_{lab}$ (degrees)